

# Interpretation of GaAs(110) scanning tunneling microscopy image contrast by the symmetry of the surface Bloch wave functions

N. D. Jäger and E. R. Weber

Materials Sciences Division, Lawrence Berkeley National Laboratory and Department of Materials Science, University of California at Berkeley, Berkeley, California 94720

M. Salmeron<sup>a)</sup>

Materials Sciences Division, Lawrence Berkeley National Laboratory, University of California, Berkeley, California 94720

(Received 27 July 2000; accepted 2 January 2001)

A simple qualitative correlation between the corrugation anisotropy observed in scanning tunneling microscope (STM) images of GaAs(110) surfaces and the symmetry properties of the surface states is presented. We show that as a function of bias, tunneling from different electronic states near high-symmetry points of the surface Brillouin zone gives rise to a distinct corrugation along  $[\bar{1}10]$  and  $[001]$  in STM images. Existing models of the surface band structure are used to identify these states. We show that at small bias, due to band bending effects, the same surface state near the conduction-band edge determines the image corrugation in both filled and empty states images of *n*-type GaAs. © 2001 American Vacuum Society. [DOI: 10.1116/1.1350839]

## I. INTRODUCTION

The (110) surface of most zinc-blende III–V compound semiconductors is interesting due to its simple  $(1\times 1)$  relaxation in conjunction with its surface-state energies being outside the fundamental bulk band gap. Thus, bulk-related features are not obstructed for scanning tunneling microscopy (STM) to probe and allows detecting features several layers deep into the bulk, such as shallow dopants and deep-level defects.<sup>1,2</sup> The surface relaxation, which consists primarily of a bond-length conserving outward rotation of the anion,<sup>3</sup> is driven by a rehybridization of atomic orbitals on the cations and anions from  $sp^3$  in the unreconstructed surface to  $sp^2$  and to  $s^2p^3$ , respectively. It is accompanied by a charge redistribution from the half-filled cation dangling bond to the half-empty anion dangling bond. With this relaxation, the energetically midgap anion dangling-bond states are pushed downward into the valence band, while the cation dangling-bond states are pushed up into the conduction band.<sup>4</sup> The charge redistribution explains the common observation that, depending on the bias polarity, either the group-III or group-V sublattice is imaged with STM. For positive sample bias electrons tunnel from the tip empty cation-derived surface states located in the conduction band (CB). Thus, the group-III sublattice is imaged. For sufficiently large negative sample bias the electrons tunnel from the filled anion-derived surface states, which energetically are in the valence band (VB), to the tip. Thus, the group-V sublattice is imaged. This behavior was first predicted by Tersoff and Hamann<sup>5,6</sup> and confirmed for GaAs(110) by Feenstra *et al.*<sup>7</sup>

Besides the polarity, STM images of the (110) surface of GaAs and other III–V compounds also depend on the magnitude of the applied bias. Efforts to explain the morphology seen at different bias voltages were made first by Möller and co-workers.<sup>8,9</sup> A short description of the connection between

the image corrugation and the surface electronic-state symmetry was presented recently by us.<sup>10</sup> More recently Ebert *et al.*<sup>11</sup> compared experimental images to *ab initio* calculations of contours of constant charge density and thereby identified the surface states involved in the tunneling.

In this article, we will show a set of experimental results on the anisotropy of the image corrugation of GaAs(110) and its dependence on bias voltage. We will present a simple analysis that illustrates how the high corrugation seen along  $[\bar{1}10]$  and  $[001]$  can be simply explained as an effect of the symmetry of the wave functions near high-symmetry points of the surface Brillouin zone. We will show that for *n*-doped samples, the structure and registry of the images acquired at sufficiently low bias are independent of bias polarity, indicating that the same electronic state of the sample near the conduction-band edge is imaged in these conditions.

## II. EXPERIMENT

Highly doped *n*-type GaAs samples were cleaved in ultra-high vacuum. The exposed (110) surface was then probed with a Walker-type STM.<sup>12</sup> Chemically etched platinum wires were used as tips. The images presented are all taken in topographic mode at a constant current at 1 nA. In the following, all polarities are given with respect to the sample.

To study the dependence of image contrast on bias, several series of images were acquired. A series is defined as a set of images acquired at different bias voltages with the same identical tip. Unfortunately, the state of the tip is not preserved indefinitely due to uncontrolled changes. These changes occur most often in the limits of high bias (large electric fields), or close proximity to the surface which occurs at the lowest bias. The acquisition of a series was terminated whenever either of these limits lead to a change of the tip structure. Such a change is observed as a discontinuity in the image. The higher limit is, typically, around 3 V (of either sign), while the low limit is around 0.5 V (for 1 nA).

<sup>a)</sup>Electronic mail: salmeron@stm.lbl.gov

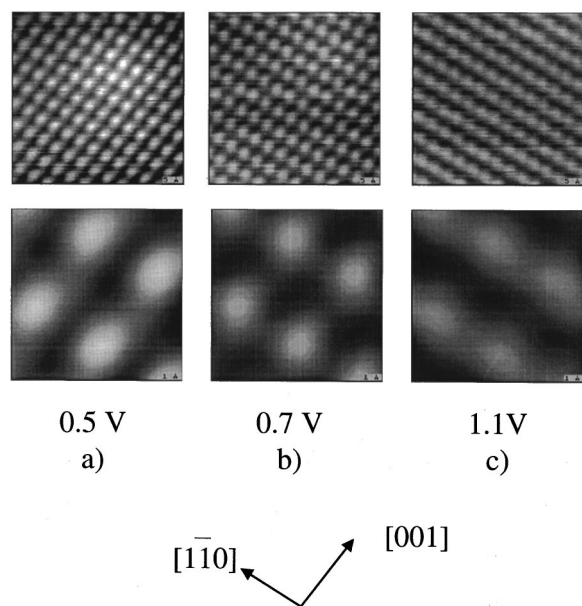


FIG. 1. Top row: STM images of *n*-type GaAs(110) at various positive sample bias voltages that show a change of symmetry and corrugation. Bottom row: STM image of one unit cell obtained by averaging over all cells in the image above. (a) Image taken at 0.5 V, showing a strong corrugation along  $[1\bar{1}0]$ . (b) Image taken at 0.7 V showing about equal corrugations along  $[001]$  and  $[1\bar{1}0]$ . (c) Image taken at 1.1 V, showing a strong corrugation along  $[001]$ .

The corrugation of the images was measured as a function of bias along the two principal crystallographic directions:  $[001]$  along the long side of the unit cell, and  $[1\bar{1}0]$  along the short side of the unit cell. The corrugation was determined by integrating the intensity of the reciprocal space peaks in the two-dimensional Fourier transform.

We also studied the changes of registry of the maxima in images taken at different polarity. To that effect, a negative bias was applied during the first third of an image, then switched to positive polarity, and after another third changed back to negative polarity. The third part of the image always completely matched the extrapolated first part. Thus, we can reasonably assume that the tip did not alter with the change of polarity.

### III. RESULTS

#### A. Bias dependence of the corrugation

In Fig. 1 we show three selected empty states STM images of *n*-GaAs taken from a series in which the bias voltage was decreased from +2.6 to +0.5 V. For clarity the lower row of images is an average computed of all unit cells in the corresponding upper image. The images illustrate the changes of morphology which can be grouped into the three distinct shapes shown in Fig. 1. At low bias, the image morphology reveals rows of maxima aligned along the  $[001]$  direction, i.e., a stronger corrugation in the  $[1\bar{1}0]$  direction [Fig. 1(a)]. At intermediate voltages individual maxima are revealed due to a similar corrugation along both crystallographic directions [Fig. 1(b)]. Finally, at high voltages the

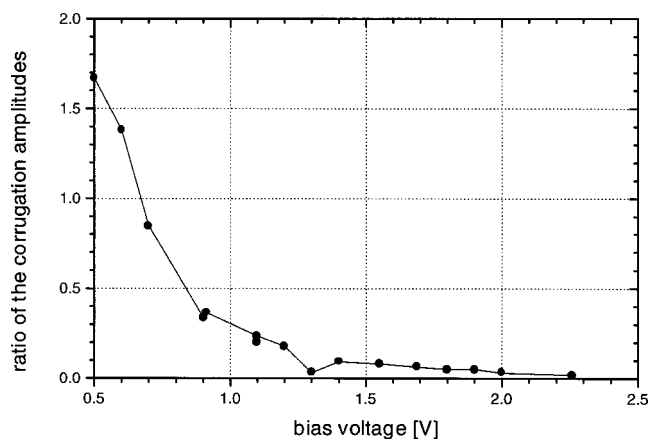


FIG. 2. Ratio of the corrugations measured along  $[1\bar{1}0]$  and  $[001]$  of Fig. 1.

images show rows aligned along  $[1\bar{1}0]$ , i.e., the corrugation is strong along  $[001]$  [Fig. 1(c)]. The ratio of the measured corrugation amplitudes as function of positive sample voltage is given in Fig. 2 for this series. With the exception of one series (possibly due to undetected tip changes) the image morphology always followed the same trend: with increasing bias the corrugation is strong first along  $[1\bar{1}0]$ , then about equally strong for both lattice directions, and at higher voltages the corrugation along  $[001]$  is stronger than along  $[1\bar{1}0]$ . Although this trend is well preserved from series to series, the magnitude changes and the point of equal corrugation shifts in voltage as high as 1 V for different series. The changes are ascribed to different tunneling conditions, such as different bandbending due to changing tip work functions with different tip apex.

The results of similar experiments performed at negative sample bias are as follows. At high voltages, between  $-3$  and  $-2$  V, the images show a relatively strong corrugation along the  $[001]$  direction, which is manifested by strings of maxima aligned along  $[1\bar{1}0]$ . This is shown in the image of Fig. 3(a). As the bias continues to decrease below  $-2$  V, the corrugation along  $[1\bar{1}0]$  increases rapidly and the images have a “zigzag” or asymmetric appearance, as shown in Fig. 3(b). The ratio of the corrugations along  $[1\bar{1}0]$  and  $[001]$  reaches a maximum around  $-1.4$  V, giving rise to images with rows aligned along  $[001]$ . The evolution of the corrugations is shown in Fig. 4.

#### B. Registry of maxima in filled and empty states images

The relative registry of the lattice of maxima in the images acquired at positive (empty states) and negative bias (filled states) was found to display interesting changes as a function of voltage. Two extreme cases were found. At high negative voltages the maxima in the two polarities are shifted along  $[001]$  and  $[1\bar{1}0]$ , as shown in Fig. 5(b), more or less as expected from the shift in the Ga and As sublattices. However, at sufficiently low negative bias voltage no difference in registry is apparent between the section of the image taken at negative voltage and the section taken at positive voltage,

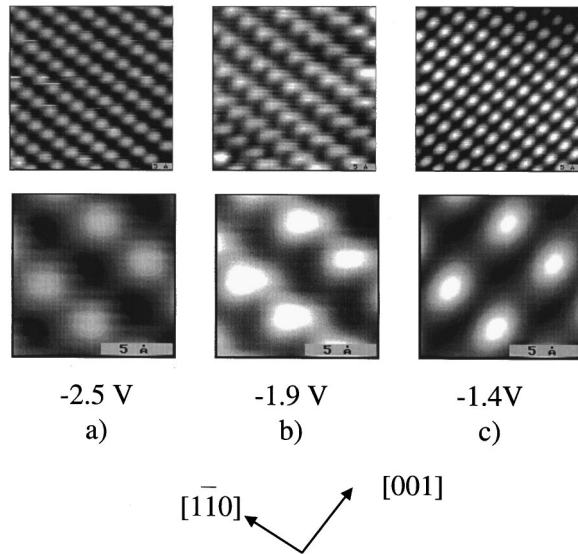


FIG. 3. Top row: STM images of *n*-type GaAs(110) at various negative bias voltages that show a change of symmetry and corrugation. Bottom row: STM image of one unit cell obtained by averaging over all cells in the image above. (a) Image taken at  $-2.5$  V, showing a strong corrugation along  $[001]$ . (b) Image taken at  $-1.9$  V showing the zigzag chain as As and Ga along  $[110]$ . (c) Image taken at  $-1.4$  V showing a strong corrugation along  $[110]$ .

as shown in Fig. 5(a). Note that the images in Fig. 5 were taken on a different sample and with a different tip than those of Figs. 1 and 3. Therefore, the orientation changed and the low-voltage limit at which rows along  $[001]$  appear.

#### IV. DISCUSSION

Before we identify the states imaged for the various bias conditions in our case of GaAs(110), we present a more general concept of how to correlate corrugation anisotropy and symmetry by the structure of surface wave functions.

##### A. Symmetry of the surface-state wave functions

We adopt the point of view that the tunneling probability is proportional to the overlap of electronic wave functions at the tip and at the surface, as done in all theoretical models of

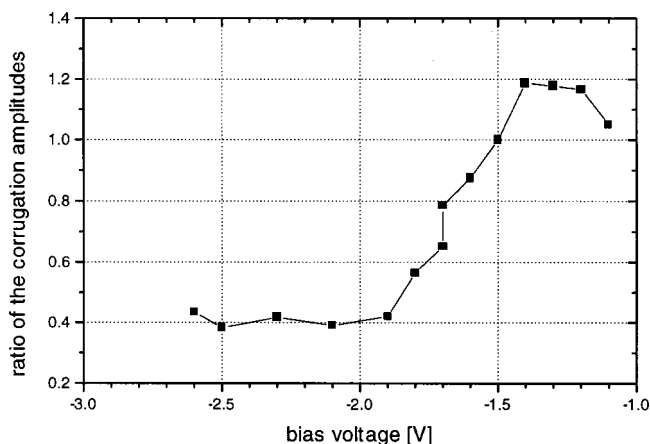


FIG. 4. Ratio of the corrugations measured along  $[110]$  and  $[001]$  of Fig. 3.

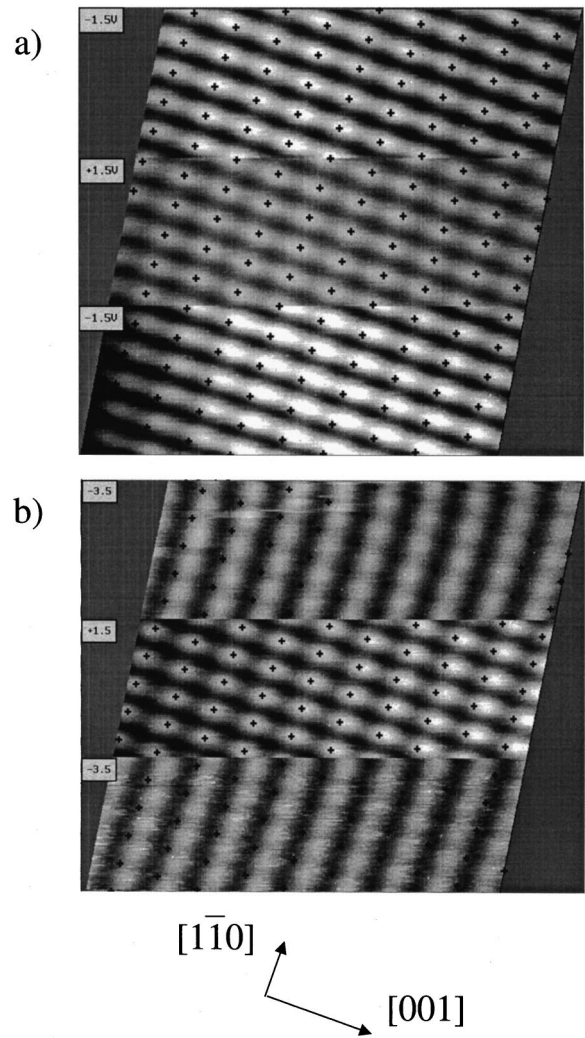


FIG. 5. STM images of GaAs(110) at varying bias. The top and bottom part of the images are taken at negative, the central part at positive sample polarity. A flat background plane is subtracted from each section to enhance the contrast of the corrugation. (a) Image taken at  $-1.5$  V/ $+1.5$  V/ $-1.5$  V; there is no registry or symmetry difference between the two polarities; the corrugation is strong along  $[110]$ . (b) Image taken at  $-3.5$  V/ $+1.5$  V/ $-3.5$  V; there is a clear shift of maxima along  $[001]$  and  $[110]$  between the two polarities, as well as a definite change in the symmetry.

tunneling. For symmetric wave functions at the tip, for example, an *s*-wave function, as assumed by Tersoff and Hamann,<sup>5,6</sup> but more generally also for  $p_z$ ,  $d_{z^2}$ , etc.,<sup>13</sup> the overlap, and therefore the tunnel current, reflects the symmetry of the surface wave function. The details of the actual wave functions depend on the theoretical model used. Using the Bardeen approximation,<sup>14</sup> which assumes that the tip-surface interaction does not modify the electronic structure, Tersoff and Hamann<sup>5,6</sup> showed that the tunneling probability is directly proportional to the sum of the modulus square of the surface wave functions at the Fermi energy, i.e., the density of states, at the tip position. Other models, including the elastic scattering quantum chemistry (ESQC) of Sautet and Joachim,<sup>15</sup> do not impose this restriction and electronic wave functions of tip and surface are obtained by solving the tip-surface Hamiltonian using a basis of atomic orbitals and



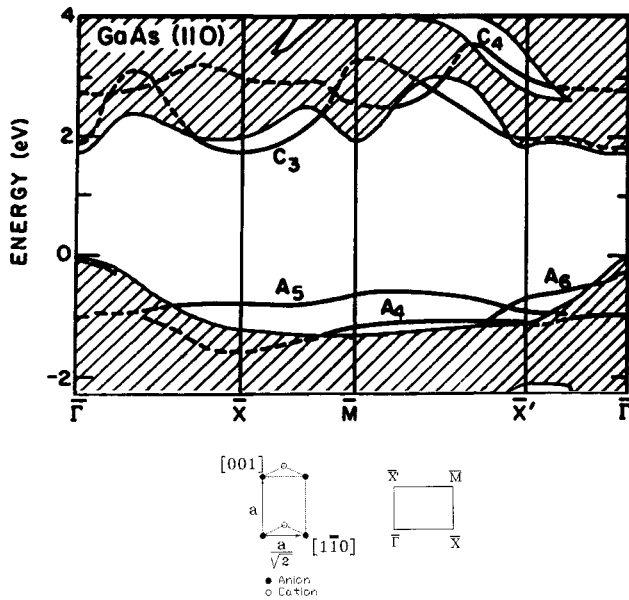


FIG. 6. Surface band structure of GaAs(110) (dashed lines) projected on the bulk bands (solid lines). [Reproduced from Ref. 16 with permission from Elsevier Science and the authors.]

the extended Hückel approximation. Here, we will assume that the interactions do not modify substantially the surface wave functions (i.e., in the limit of weak interaction), and in particular, that their symmetry is preserved.

In order to facilitate the discussion, we reproduce in Fig. 6 the band structure of GaAs projected on the (110) surface, taken from the work of Chelikowsky and Cohen.<sup>16</sup> Other more recent calculations,<sup>17–19</sup> notably that of Alves, Hebenstreit, and Scheffler,<sup>20</sup> essentially confirm the structure. In Fig. 6 only bands near the fundamental band gap are shown. Notice, in particular, the bands from the most external states, including dangling bonds close to the band edges, marked  $C_3$  and  $A_5$ , and back bonds  $C_4$  and  $A_4$ . Because these states will overlap most efficiently with the tip, they are expected to be the largest contributors to the tunneling current. In contrast, and although energetically matched at the appropriate bias, bulk states (shaded part of the band structure in Fig. 6), do not overlap efficiently and are thus expected to contribute little to the corrugation. States near the  $\bar{X}$  point of the surface Brillouin zone will be connected to strong corrugations along  $[1\bar{1}0]$ , while the strong corrugation along  $[001]$  will be coupled to states near the  $\bar{X}'$  point, which can be accessed at different bias. The Bloch wave functions are of the form

$$\Psi_k(\mathbf{r}) = \sum_j \phi_a(\mathbf{r} - \mathbf{r}_j) \cdot e^{ik(\mathbf{r} - \mathbf{r}_j)}, \quad (1)$$

where  $\phi_a$  represents atomic or molecular orbitals. The symmetry of these wave functions can be easily visualized at the high symmetry points of the Brillouin zone where the exponential  $e^{ik \cdot \mathbf{r}_j}$  takes values of only +1 or -1. These points are the zone center  $\bar{\Gamma}$  and the boundary points at  $\bar{X}$ ,  $\bar{M}$ , and  $\bar{X}'$ .  $\bar{\Gamma}$  corresponds to the wave vector  $\mathbf{k} = (000)$ ;  $\bar{X}$  to  $\mathbf{k} = (\sqrt{2}\pi/a) \times (1\bar{1}0)$ ;  $\bar{X}'$  to  $\mathbf{k} = (\pi/a)(001)$ ; and  $\bar{M}$  to  $\mathbf{k} = (\sqrt{2}\pi/a) \times (11\sqrt{2}/2)$ . This is shown schematically in Fig. 7.

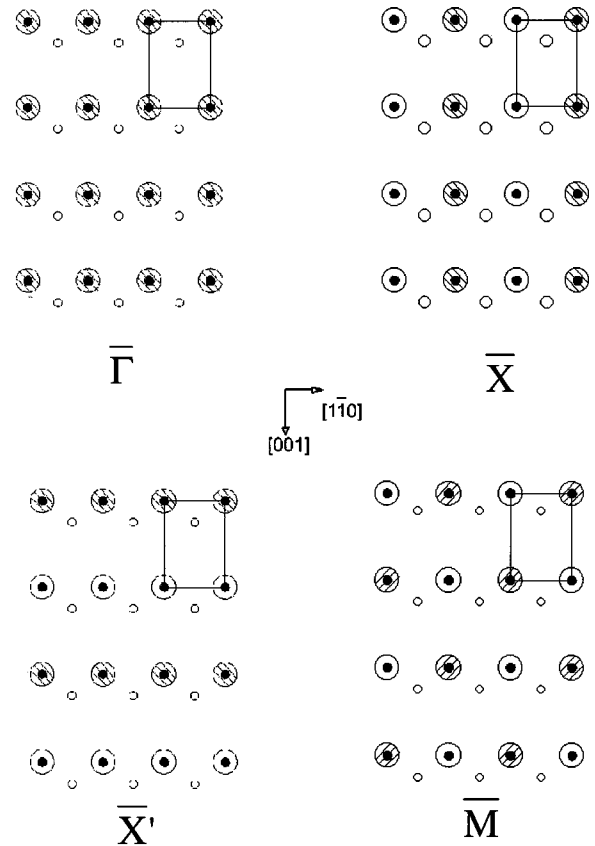


FIG. 7. Illustration of empty surface states at high symmetry points  $\bar{\Gamma}$ ,  $\bar{X}$ ,  $\bar{M}$ , and  $\bar{X}'$ , of the (110) surface Brillouin zone. Cations can be assumed to be located on the lattice points marked  $\bullet$ ; corresponding positions of the anions are marked  $\circ$ . The circles around the lattice points represent atomic orbitals. They are drawn open or shaded depending on whether the multiplying factor  $e^{ik \cdot \mathbf{r}_j}$  of their Bloch wave function is +1 or -1.

In Fig. 7, cations can be assumed to be located on the lattice points marked  $\bullet$ . Corresponding positions of the anions are marked  $\circ$ . The circles around the lattice points correspond to atomic orbitals  $\phi_a(\mathbf{r} - \mathbf{r}_j)$ . They are drawn open or shaded depending on whether the multiplying factor  $e^{ik \cdot \mathbf{r}_j}$  is +1 or -1. It is clear that  $\Psi_k(\mathbf{r})$  has nodal points along  $[001]$  for states near  $\bar{X}'$ , along  $[110]$  for states near  $\bar{X}$ , and along both lattice directions for states near  $\bar{M}$ . It has no nodes for states near  $\bar{\Gamma}$ . The presence of nodes indicate that the tunneling probability will vanish if the tip is located between lattice points, giving rise to strong corrugation along the corresponding direction when the tunneling bias matches the energy of the states. If there are no nodes, but a mirror symmetry halfway between lattice points, the corrugation along this direction is expected to be weaker.

## B. Analysis of the dependence on bias voltage

For the GaAs(110) surface the surface states are energetically outside the band gap. Thus, the surface is often presumed unpinned, i.e., not exhibiting a surface potential. In this case, a close proximity of a metallic tip would induce local bandbending. At zero bias we expect a surface potential of about 1 eV for a sample doping level of  $1 \times 10^{18} \text{ cm}^{-3}$

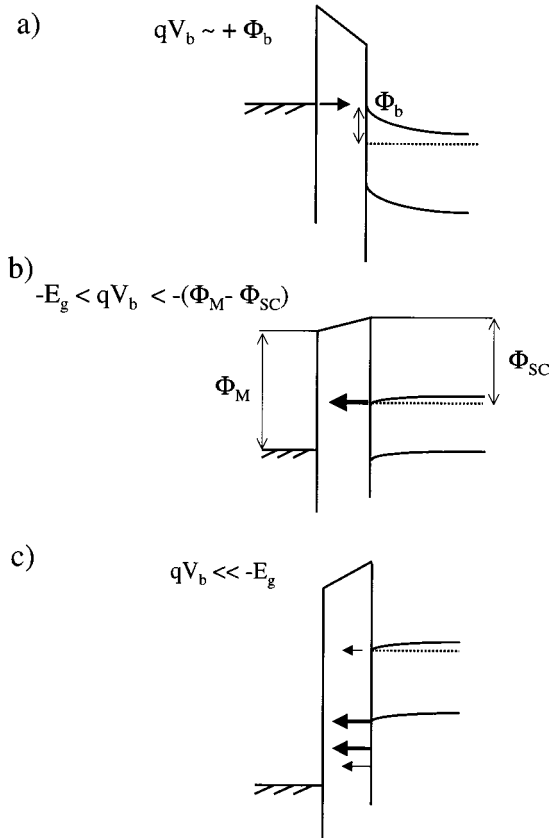


FIG. 8. Band diagram of the metal tip/n-type GaAs system at (a) a sample bias, where tunneling just starts to occur into the lowest states directly at the semiconductor surface. The surface is assumed to be pinned by extrinsic states reducing the effect of tip-induced band bending to  $\Phi_b$ . (b) For a sample bias from 0 to  $-E_g$ , the band-gap energy, the tip Fermi level falls into the semiconductor band gap. Electrons in conduction-band states are expected to tunnel, if these are filled due to carrier accumulation at a bias voltage sufficient to flatten the bands:  $qV_b < -(\Phi_M - \Phi_{SC})$ , where  $\Phi_M$  and  $\Phi_{SC}$  are the metal and semiconductor work functions, respectively. (c) At higher negative voltages the tunneling current consists of electrons tunneling from the conduction and valence bands.

and an assumed tip-sample distance of 0.9 nm.<sup>21</sup> Raising the tip Fermi level by applying a positive voltage to the sample would increase the bandbending. For an unpinned noninverting surface the tip Fermi level is expected to rise above the bottom of the conduction band for bias voltages of at least 6 V. If the surface would invert, raising the tip Fermi level by 1.5 V brings it above the bottom of the conduction band. Any current seen at bias voltages below 1.5 V thus consists of electrons tunneling not directly into the surface, but through the space-charge region into bulk states.<sup>21</sup> Bulk states are not expected to show a strong corrugation of their density of states at the position of the tip apex. However, we observe a strong corrugation for voltages as low as 0.5 V, implying that the tunneling current is spatially modulated by surface states. Since surface states reside outside the band gap, bandbending must have been pinned to about 0.5 V to allow tunneling into these states at these relatively low voltages [see Fig. 8(a)]. Extrinsic states, such as cleavage steps, adsorbates, and vacancies, may have pinned the surface.<sup>22</sup> The lowest surface band that electrons can tunnel into is  $C_3$

(see Fig. 6), which is essentially the cation dangling bond. This band has a distinct minimum near the  $\bar{X}$  point of the surface Brillouin zone. As explained above, states near  $\bar{X}$  are expected to show a strong corrugation along  $[1\bar{1}0]$ , which is indeed seen in the images [Fig. 1(a)].

With increasing bias, states further away from the  $\bar{X}$  point also contribute to the tunneling, and thus the corrugation along  $[1\bar{1}0]$  must become weaker (Fig. 2). Eventually states near  $\bar{\Gamma}$ ,  $\bar{M}$ , and  $\bar{X}'$  will also contribute appreciably so that the corrugation along both lattice directions will become similar. With further increases in voltage, states from the  $C_4$  band will be accessed. Experimentally, we observe a strong corrugation always along  $[001]$  for high voltages [Figs. 1(c) and 2]. This points to states near  $\bar{X}'$ , for which Chadi<sup>4</sup> predicts a large  $p_y$  orbital component (i.e., back bonds) which has a less favorable spatial distribution for overlap with the tip and a smaller  $p_z$  (outward pointing) component. It might be that this smaller  $p_z$  component is still sufficient to explain the observations, but we cannot reach this conclusion based on the symmetry arguments alone. In the recent calculations of Ebert *et al.*<sup>11</sup> the image corrugation at large bias is indeed attributed to the back bonds.

In Fig. 5 we show that the negative bias images fall into two categories. For low negative bias, between about  $-1$  and  $-1.6$  V, filled state images show a strong corrugation along  $[1\bar{1}0]$  and the rows of maxima do not shift with respect to the part of the image taken at low positive bias ( $+1.5$  V). In images with high negative bias (between  $\sim -2$  and  $-4$  V), however, we see the commonly observed shift of the maxima [Fig. 5(b)]. One has to bear in mind that for bias between 0 and  $-1.5$  the top Fermi level is in the band-gap region. The fact that the contrast is virtually identical for positive and negative bias in Fig. 5(a) suggests that under these conditions tunneling occurs in and out of the same surface states. Above, we identified states near the  $\bar{X}$  minimum in the  $C_3$  band causing the strong corrugation along  $[1\bar{1}0]$  for low positive voltage. We conclude that tunneling out of these conduction-band states also occurs at low negative bias. They become filled due to carrier accumulation in the tip-induced downward-bent conduction band [Fig. 8(b)]. Accumulation is expected for negative bias exceeding the flat-band condition  $qV_{FB} = -(\Phi_M - \Phi_{SC})$ , where  $\Phi_M$  is the metal and  $\Phi_{SC}$  is the semiconductor work function. Assuming the semiconductor work function is within 100 meV of the electron affinity (4.07 eV), the flat-band condition bias is expected to be at a voltage between 0 and  $-1.6$  V for tip work functions ranging from 4 to 5.65 eV.

When the tip Fermi level is below the top of the valence band, i.e., for a bias  $< -1.5$  V, states that are energetically in the valence band contribute to the tunneling current as well [Fig. 8(c)]. For high negative bias the images always show a stronger corrugation along  $[001]$ , as seen in Figs. 3(a), 4, and 5(b). This can be understood if tunneling occurs primarily out of states near  $\bar{M}$  and  $\bar{X}'$  in the valence band. The highest filled states (and those extending farthest out of the surface) are the anion dangling bond and the bank bond, which form the bands labeled  $A_5$  and  $A_4$  in Fig. 6. They are strong at  $\bar{X}'$ .<sup>4</sup>

The dangling bond has the higher density of states<sup>4,16</sup> and is spatially favored (nearest to the tip), and thus probably dominates. However, since the energy dispersion of these filled surface states is relatively small (their entire dispersion has only a range of less than 0.4 eV), it is difficult to predict which Brillouin zone states would dominate the tunneling.

Theoretically, we would expect that at certain bias an about equal amount of electrons tunnel from states in the valence band and from states in the conduction band. Thus, one would expect some kind of transition region, in which cation- and anion-derived states are visible. In the series shown in Fig. 3 the image taken at about  $\sim -1.9$  V shows a zigzag chain structure and could thus correspond to this transition.

A simultaneous appearance of the arsenic and gallium sublattices has previously been addressed briefly by us<sup>10</sup> and Heinrich *et al.*<sup>23</sup> These results were obtained on *p*-type GaAs and very low bias, which is equivalent to small tip-sample separations. The images show individual arsenic and gallium "atoms" of about equal strength. Based on a significant reduction of the tip-sample separation, Heinrich *et al.* proposed that tip-induced modifications of the surface states cause these phenomena. We will address this issue in a separate publication,<sup>24</sup> because the clear simultaneous appearance seen at small tip-sample separation may not be related to the phenomenon seen in Fig. 3(b), where the tip-sample distance lies between the tip-sample distance of  $-1.4$  and  $-2.5$  V, and is thus not significantly reduced.

## V. SUMMARY

We have acquired a series of STM images on the GaAs(110) surface that show a clear dependence of the corrugation and registry of the maxima as a function of bias. Using simple symmetry arguments the corrugation seen in the images is assigned to tunneling processes dominated by surface states near high-symmetry points of the surface Brillouin zone. Existing band-structure calculations were utilized to identify these states. For low bias (positive or negative) and for *n*-type samples, empty Ga dangling bond states near  $\bar{X}$  dominate the structure of the image. For higher positive voltages, states near  $\bar{X}'$  determine the image structure with contributions from both dangling- and back-bond states. For high negative sample bias, the more localized, filled As dangling-bond states dominate the image. We have also shown that due to band-bending effects CB states are accessed at both polarities for low voltages, which is contrary to the common opinion that only VB states can be seen at negative sample bias. The near independence of the image structure on the sign of the bias for low voltages ( $|V| < \sim 1.5$  V) indicates that the same surface states (Ga dangling-bond states near the  $\bar{X}$  point) determine the image structure. We believe that these arguments might also be applied to STM images of other III-V semiconductor surfaces.

More elaborate studies on the corrugation as a function of bias were recently presented by Ebert *et al.*<sup>11</sup> The authors used *ab initio* local density of states calculations which show

that the most important states involved in the tunneling, that determine the image structure, are those derived from the dangling- and back-bond states. We arrived at a similar conclusion, albeit in a qualitative way, by simple symmetry considerations of the surface states and their Bloch wavefunction combinations at the surface Brillouin zone. We have shown that this is sufficient for a qualitative understanding of the structure and corrugation changes of the tunneling images. This interpretation of the images stresses the physical origin of the tunneling current.

## ACKNOWLEDGMENT

This work was supported by the Director, Office of Energy Research, Office of Basic Energy Research, Materials Science Division, U.S. Department of Energy under Contract No. DE-AC03-76SF00098.

<sup>1</sup>J. F. Zeng, J. D. Walker, M. B. Salmeron, and E. R. Weber, Phys. Rev. Lett. **72**, 2414 (1994).

<sup>2</sup>R. M. Feenstra, J. M. Woodall, and G. D. Pettit, Phys. Rev. Lett. **71**, 1176 (1993).

<sup>3</sup>A. R. Lubinsky, C. B. Duke, B. W. Lee, and P. Mark, Phys. Rev. Lett. **36**, 1058 (1976).

<sup>4</sup>D. J. Chadi, Phys. Rev. B **18**, 1800 (1978).

<sup>5</sup>J. Tersoff and D. R. Hamann, Phys. Rev. Lett. **50**, 1998 (1983).

<sup>6</sup>J. Tersoff and D. R. Hamann, Phys. Rev. B **31**, 805 (1985).

<sup>7</sup>R. M. Feenstra, J. A. Stroscio, J. Tersoff, and A. P. Fein, Phys. Rev. Lett. **58**, 1192 (1987).

<sup>8</sup>R. Moller, C. Baur, A. Esslinger, U. Graf, and P. Kurz, Nanotechnology **1**, 50 (1990).

<sup>9</sup>R. Moller, J. Fraxedas, C. Baur, B. Koslowski, and K. Dransfeld, Surf. Sci. **269-270**, 817 (1992).

<sup>10</sup>N. D. Jäger *et al.*, in *23rd International Conference on the Physics of Semiconductors*, edited by M. Scheffler and R. Zimmermann (World Scientific, Berlin, Germany, 1996), Vol. 2, p. 847.

<sup>11</sup>P. Ebert *et al.*, Phys. Rev. Lett. **77**, 2997 (1996).

<sup>12</sup>J. Frohn, J. F. Wolf, K. Besocke, and M. Teske, Rev. Sci. Instrum. **60**, 1200 (1989).

<sup>13</sup>N. D. Lang, Phys. Rev. Lett. **56**, 1164 (1986).

<sup>14</sup>J. Bardeen, Phys. Rev. Lett. **6**, 57 (1961).

<sup>15</sup>P. Sautet and C. J. Joachim, Phys. Rev. B **38**, 12238 (1988).

<sup>16</sup>J. R. Chelikowsky and M. L. Cohen, Solid State Commun. **29**, 267 (1979).

<sup>17</sup>A. Zunger, Phys. Rev. B **22**, 959 (1980).

<sup>18</sup>C. Mailhot, C. B. Duke, and D. J. Chadi, Phys. Rev. B **31**, 2213 (1985).

<sup>19</sup>X. Zhu, S. B. Zhang, S. G. Louie, and M. L. Cohen, Phys. Rev. Lett. **63**, 2112 (1989).

<sup>20</sup>J. L. A. Alves, J. Hebenstreit, and M. Scheffler, Phys. Rev. B **44**, 6188 (1991).

<sup>21</sup>R. M. Feenstra and J. A. Stroscio, J. Vac. Sci. Technol. B **5**, 923 (1987).

<sup>22</sup>W. E. Spicer, I. Lindau, P. E. Gregory, C. M. Garner, P. Pianetta, and P. W. Chye, J. Vac. Sci. Technol. **13**, 780 (1976).

<sup>23</sup>A. J. Heinrich, M. Wenderoth, M. A. Rosentreter, M. A. Schneider, and R. G. Ulbrich, Appl. Phys. Lett. **70**, 449 (1997).

<sup>24</sup>N. D. Jäger *et al.* (unpublished).